Processing and Application of Ceramics 18 [4] (2024) 348–356
https://doi.org/10.2298/PAC2404348K

Magnetically tailored dielectric behaviour of (1-x)$Ba_{0.98}Sm_{0.02}TiO_3$-$xBa_{0.7}Sr_{0.3}Fe_{12}O_{19}$ ceramic composites

Arshdeep Kaur[1], Amritpal Singh Nindrayog[2], Sajan Masih[1], Shiffali Middha[1], Shubhpreet Kaur[3], Sunil Kumar[4], Rubina Ghosh[5], Prakash Nath Vishwakarma[5], Nisharika Arya[6], Satvir Singh[6], Nitin Tandon[6], Indu Sharma[7], Vishal Arora[8], Surinder Paul[9], Mandeep Singh[1], Vibha Chopra[10], Anupinder Singh[1,*]

[1]*Guru Nanak Dev University, Dept. Physics, Amritsar, Punjab, 143005, India*
[2]*Lyallpur Khalsa College, Dept. Physics, Jalandhar, 144001, India*
[3]*National Institute of Technology, Dept. Physics & Photonics, Hamirpur, Himachal Pradesh, 177001, India*
[4]*Sardar Beant Singh State University, Dept. Applied Physics, Gurdaspur, Punjab, 143521, India*
[5]*National Institute of Technology, Sector 1, Dept. Physics and Astronomy, Rourkela, Odisha 769008, India*
[6]*CT University, Dept. Applied Sciences, Ludhiana, Punjab 142024, India*
[7]*Career Point University, Dept. Physics & Center for Green Energy Research, Hamirpur, Himachal Pradesh, 176041, India*
[8]*Hindu College, Dept. Physics, Amritsar, Punjab, 143001, India*
[9]*Central University of Himachal Pradesh, Dept. Physics and Astronom. Science, Dharmshala 176215, India*
[10]*Gurugram University, Dept. Physics, Mayfield Gardens, Sector 51, Gurugram Haryana, 122018 India*

Received 14 June 2024; Received in revised form 5 July 2024; Received in revised form 22 October 2024; Accepted 6 November 2024

Abstract

With the growing need for materials for multifunctional devices, we are studying the behaviour of a composite consisting of titanate ferroelectric phase with strong dielectric properties and ferrites with magnetic properties. Solid-state reaction method was used to prepare $Ba_{1-x}Sm_xTiO_3$ powders, while $Ba_{1-x}Sr_xFe_{12}O_{19}$ powders were synthesized by sol-gel auto combustion method. The selected titanate and M-type hexaferrite powders were used for fabrication of (1-x)$Ba_{0.98}Sm_{0.02}TiO_3$-x$Ba_{0.7}Sr_{0.3}Fe_{12}O_{19}$ composites (x = 0.1, 0.2, 0.3, 0.4, and 0.5) by their mixing, compaction and sintering at 1240 °C. Phase formation was investigated by XRD and multivalent state of Fe (Fe^{2+} and Fe^{3+}) was identified from XPS. Matching the unique properties of these materials with each other will favour numerous application paths. The magnetic, magneto-dielectric and magnetoelectric properties of perovskite/hexaferrite composites were investigated. Magnetoelectric coupling was found in all of the composite samples by the magneto-dielectric investigation. The maximum magneto-dielectric response of ~37.7% in terms of change in dielectric permittivity in presence of magnetic field was measured for the sample with x = 0.4 at magnetic field of 1.2 T and frequency of 100 Hz.

Keywords: *multiferroics, hexaferrite, magnetoelectric coupling, magneto-dielectric response*

I. Introduction

Multiferroic materials are those in which both ferroelectric and magnetic orders coexist and are coupled. The mutual coupling between these orders is known as magnetoelectric (ME) coupling. This coupling allows for the manipulation of magnetization using an electric field and the control of electric polarization with a magnetic field [1]. The direct magnetoelectric effect, or magnetoelectric response, refers to the generation of an electric polarization when a magnetic field is applied. Accordingly, the converse ME effect is observed when a

*Corresponding author: +91 9988191852
e-mail: *anupinders@gmail.com*

magnetization arises after applying an electric field [2]. Ferroelectricity is typically associated with transition metals having a configuration of d^0 (e.g. Ti^{4+}), while the magnetic order is governed by transition metals with a configuration of d^n (e.g. Fe^{3+}) [3]. At room temperature, single phase materials do not combine significant and persistent electric and magnetic polarizations. The difficulties of integrating electrical and magnetic ordering in a single phase have been avoided by establishing two-phase composite multiferroics. The magnetoelectric effect in such composites is caused by the combination of the elastic components of the ferromagnetic and ferroelectric constituents. An electric field generates strain in the ferroelectric, which is then transferred to the ferromagnet, where it causes magnetization. If the coupling at the interface is high, the magnetoelectric effect is high [4]. Magnetic and electrical properties in two-phase materials are strain-coupled by arrangement in search of substantial magnetoelectric effects [5]. Van Suchetelene was the first to propose the ME effect in composite materials as a result of the idea of product property which is missing in the constituent phases [6]. When a magnetic field is applied to a composite of the piezoelectric perovskite and spinel structure phase, the ferrites change form due to the magnetostriction, and the strain is transferred on to the piezoelectric particles, resulting in electric polarization [7].

This paper describes a method for producing a substantial ME effect with a composite material comprising of two phases: a perovskite phase known as $Ba_{0.98}Sm_{0.02}TiO_3$ (BSTO) and a spinal M-type hexaferrite phase known as $Ba_{0.7}Sr_{0.3}Fe_{12}O_{19}$ (BSFO). The technique involves applying strain on piezoelectric grains, which causes electric polarization. The magnetoelectric effect achieved in this manner can be numerous times greater than that obtained in the single-phase magnetoelectric material Cr_2O_3 [8]. To achieve better ME effects in composites, it is necessary to have high magnetostriction, high piezoelectric coefficient, high dielectric permeability, high poling strength, high molar percentage, no chemical reaction between the phases and high resistivity to prevent accumulation leakage [9].

Barium titanate ($BaTiO_3$) exhibits ferroelectric behaviour at and above room temperature ($T_c \approx 393$ K), making it a valuable and important material for technology. At the Curie temperature ($T_c \approx 120$ °C), $BaTiO_3$-based ferroelectrics switch from the paraelectric to the ferroelectric phase. This transformation typically results in a complex stress system in this ferroelectric material, which generates internal stresses at room temperature that have a substantial impact on barium titanate's characteristics [10]. After doping, larger crystallites and increased dielectric behaviour are observed. It was discovered that the dielectric constant improved compared to the undoped $BaTiO_3$, but decreased with frequency [11]. Hetero-valent substitutions like Sm^{3+} for Ba^{2+} or Ti^{4+} can result in charge imbalances, leading to the formation of vacancies on A or B sites or the creation of holes which helps to maintain electrical charge neutrality [12]. Doping with Sm^{3+} ions can lower the transition temperature to 323 K while the dielectric constant value increases to 6400. Sm-doped BT is a very attractive material for many different kinds of applications, including piezoelectric actuators, FeRAM and microwave devices, particularly in the telecommunications industry [13].

On the other hand, the ferrimagnetic M-type Ba-hexaferrites have been employed in applications like anti-electromagnetic interference coatings, microwave absorbing paints, magnetic recording and gyromagnetic devices, due to their high saturation magnetization, cheap synthesis cost, high resistivity and tunable anisotropy field [14]. Many laboratories developed these ferrites and investigated into whether dopants influenced the magnetic characteristics of these M-type magnetic hexaferrites. Trukhanov *et al.* [15] investigated the impact of gallium doping on the characteristics of the ceramically manufactured barium hexaferrite, $BaFe_{12-x}Ga_xO_{19}$ ($x = 1.2$). They demonstrated that these Ga doped hexaferrites are capable of absorbing high-frequency electromagnetic radiation and that the unit cell monotonically diminishes with increasing content of Ga. Similarly, $Ba_{1-x}Sr_xFe_{12}O_{19}$ was selected for this investigation because of its high magneto-crystalline anisotropy and to a greater extent stable structure [16]. Strontium doped barium hexaferrite exhibit high magnetic properties with relatively high resistance and low dielectric losses [17]. Due to its practical application in permanent magnets and future applications in high density magnetic recording media and microwave devices, hexagonal M-type barium ferrite ($BaFe_{12}O_{19}$) and its doped compounds have attracted a lot of attention. Large crystalline anisotropy, high magnetization, strong inherent coercivity, outstanding chemical stability, high Curie temperature and low cost are all characteristics of barium hexaferrites. Barium hexaferrite has been extensively explored as one of the most significant microwave absorption materials because of its outstanding magnetic and microwave characteristics [18].

In the most single-phase multiferroic materials, such as $Bi_{0.9-x}Tb_xLa_{0.1}FeO_3$, $PbMn_xTi_{1-x}O_3$ and $Bi_{0.5}Pb_{0.5}Fe_{0.5}Ce_{0.5}O_3$, ME coupling is weak due to the opposite requirements for *d*-orbitals of transition metals. Namely, ferroelectricity arises from empty *d*-orbital or partially filled *d*-orbital, while ferromagnetism requires unpaired electrons in *d*-orbital. This limits single phase multiferroism [19–21]. However, strong ME coupling was observed in $Na_{0.5}Bi_{0.5}TiO_3$-$BaFe_{12-2x}Co_xTi_xO_{19}$, Ca-doped $BaFe_{12}O_{19}$-$Na_{0.5}Bi_{0.5}TiO_3$, and xNiFe$_2$O$_4$-(1-x)$Ba_{0.8}Sr_{0.2}TiO_3$ composites, due to integration of separate ferroelectric and ferromagnetic phase, enabling strong interaction among different domains yielding enhanced magnetoelectric coupling [22–24].

According to a survey of the literature, no investigations have been carried out on the synthesis and compre-

hensive investigation of a multiferroic composite consisting of Sm-doped $BaTiO_3$ and Sr-doped M-type Ba-hexaferrite. Thus, structure, dielectric, magnetic and magneto-dielectric properties of (1-x)$Ba_{0.98}Sm_{0.02}TiO_3$-$xBa_{0.7}Sr_{0.3}Fe_{12}O_{19}$ (where x = 0.1, 0.2, 0.3, 0.4, and 0.5) ceramics were investigated.

II. Experimental

2.1. Sample preparation

This paper is concerned with magnetic and magnetoelectric properties of a composite made of the M-type hexagonal phase of Sr-doped barium hexaferrite and Sm-doped barium titanate ferroelectric phase. High-purity raw materials, $BaCO_3$ (99.90%), Sm_2O_3 (99.90%) and TiO_2 (99.90%), were used to synthesize the series of samarium-doped barium titanate ($Ba_{1-x}Sm_xTiO_3$, x = 0.02, 0.04, 0.06, 0.08 and 0.1) by utilizing solid-state reaction approach. Stoichiometric amounts of raw materials were carefully weighed and mixed using an agate mortar and pestle in an acetone medium to ensure homogeneity. Then the ground powders were calcined for 12 h at 1000 °C.

Raw materials of $Ba(NO_3)_3$ (99.90%), $Sr(NO_3)_2$ (99.90%), $Fe(NO_3)_2 \cdot 9H_2O$ (99.98%) and citric acid ($C_6H_8O_7 \cdot H_2O$) were used to synthesize a series of strontium-doped barium hexaferrites ($Ba_{1-x}Sr_xFe_{12}O_{19}$, x = 0.1, 0.2, 0.3, 0.4 and 0.5) by using sol-gel auto combustion method. Stoichiometric amounts of raw materials were mixed the same as with Sr-doped barium titanate in agate mortar and acetone which was followed with calcination at 1200 °C for 12 h.

To synthesize multiferroic composites, the best compositions from the two series were selected. Since the dielectric permittivity of $Ba_{0.98}Sm_{0.02}TiO_3$ (BSTO) is high, it was selected as the ferroelectric (FE) component. On the other hand, the high remanent magnetization of $Ba_{0.7}Sr_{0.3}Fe_{12}O_{19}$ (BSFO) was the reason for selecting it as the ferromagnetic (FM) component. The calcined powders of the constituent phases were ground and then mixed in acetone medium for 5 h according to the formula (1-x)BSTO-xBSFO where x = 0.1, 0.2, 0.3, 0.4 and 0.5 (abbreviated as 90-10, 80-20, 70-30, 60-40 and 50-50, respectively). The binder, polyvinyl alcohol (PVA), was mixed with the powder, followed by pressing the mixture into pellet form using a hydraulic press. Sintering was carried out as the final stage at 1240 °C.

The primary focus of this work was to investigate the magnetoelectric behaviour of the composite systems with increasing $Ba_{0.7}Sr_{0.3}Fe_{12}O_{19}$ content. To the best of our knowledge, there is no such extensive report on the effect of temperature and frequency on the dielectric characteristics of Sm-doped barium titanate and Sr-doped barium hexaferrite multiferroic composites.

2.2. Characterization

X-ray diffraction (XRD) spectra of the BSTO-BFTO composites were measured at 25 °C with a X'Pert PRO, Panalytical diffractometer, The Netherlands, utilizing CuKα radiation in 2θ range from 20° and 75°. Field emission scanning electron microscope (FESEM) and energy dispersive spectroscopy (EDAX) from Carl Zeiss Supra 55, Germany were used for the surface studies and elemental analysis, respectively. Experimental densities were measured by the Archimedes principle. The presence of multivalent Fe ions as well as changes in their relative concentrations were analysed by X-ray photoelectron spectroscopy (XPS) on Omicron ESCA electron spectrometer from Oxford instruments, Germany. The magnetic hysteresis loops were obtained using vibrating sample magnetometer from Microsense, USA and magnetoelectric effect was measured in terms of the variation of the magnetoelectric coefficient as a function of magnetic field.

III. Results and discussion

3.1. Structure characteristics

XRD patterns of the parent materials BSTO and BSFO, as well as for the composite sample 50-50, are shown in Fig. 1. One can easily see that the XRD pattern of the sample 50-50 consists of peaks of both phases.

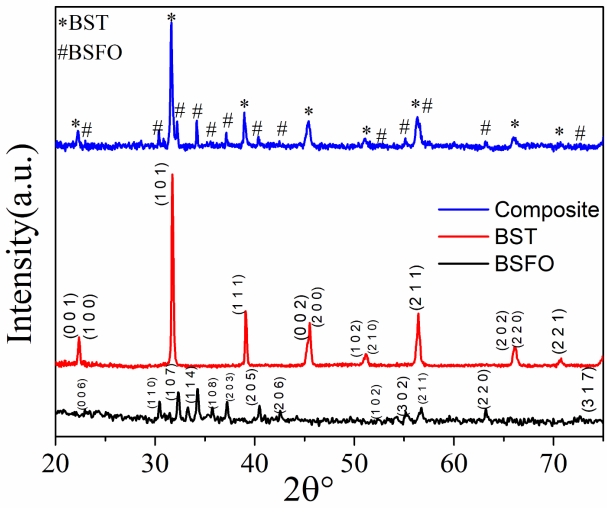

Figure 1. XRD patterns of composite sample 50-50 and the parent materials BSTO and BSFO

X-ray diffractograms of the (1-x)BSTO-xBSFO (x = 0.1, 0.2, 0.3, 0.4 and 0.5) composites are shown in Fig. 2. The high-intensity sharp diffraction peaks result from the highly crystalline nature of the prepared ceramic composites. The primary crystallographic information regarding prepared composite ceramics was retrieved by comparing experimental data with reported Joint Committee on Powder Diffraction Standards (JCPDS) cards representing particular crystallographic information for specified space group of each crystal phase.

The single-phase tetragonal configuration of BSTO [25], with space group $P4/mm$ (JCPDS card No. 05-0626), and the hexagonal structure of BSFO [26], with space group $P6_3/mmc$ (JCPD card No. 79-1411), are

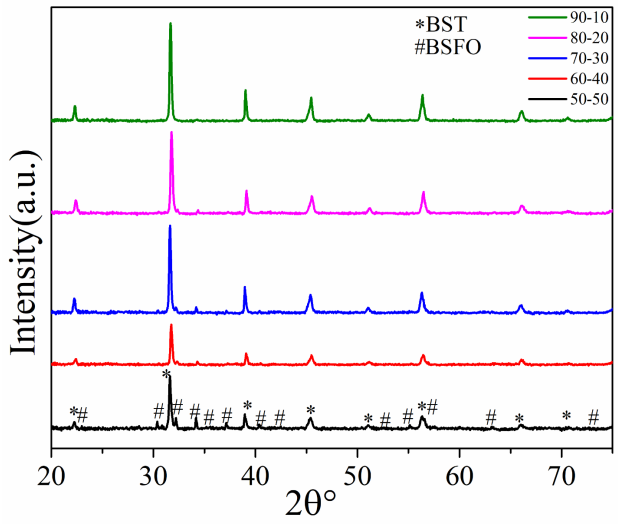

Figure 2. The XRD patterns for the composite samples (a) 90-10, (b) 80-20, (c) 70-30, (d) 60-40 and (e) 50-50

supported by the well-matched diffraction lines. XRD peaks of the BSTO phase dominate for $x = 0.1$, and this dominance decreases with rise of x value. For $x = 0.5$, reflection peaks of the BSFO counters the BSTO phase competitively.

The absence of unexplained peaks indicates that there were no chemical reactions between the hexaferrite and ferroelectric phases during the final sintering. It was discovered that as the amount of hexaferrite phase increased, so did the intensity and number of its peaks, whereas the ferroelectric phase's peaks intensity remained almost constant. The quantity of corresponding phases present in the composites determines the intensity and number of diffraction peaks.

3.2. Surface study and density

Surface morphology of the prepared ceramic composites was investigated using a FESEM (Fig. 3). FESEM images revealed the well-defined and uniformly spaced grains. The average grain size of each sample was calculated using ImageJ software. The microstructure of the sample 90-10 exhibits dominance of the round-shape grain structure. However, with increase in the value of x for the samples 80-20 to 50-50, a discernible shift to the hexagonal grains from the round ones has been observed (Fig. 3).

The interplay between doping concentrations influences the microstructure of the samples. Moreover, the decrease of average grain size and density with rise in hexagonal phase content was observed as listed in Table 1.

The data from the EDAX have confirmed the elemental occurrence for the necessary composition. Additionally, mapping for each element available has been completed to verify the element's uniform distribution. In Fig. 4 only the sample mapping and EDAX for the 90-10 composite are shown, with distinct colours denoting distinct elements.

Table 1. Density and average grain size of BSTO-BFTO composites

Sample	Grain size [μm]	Density [g cm^{-3}]
90-10	3.76	5.76
80-20	3.68	5.62
70-30	3.65	5.41
60-40	3.25	4.98
50-50	3.22	4.96

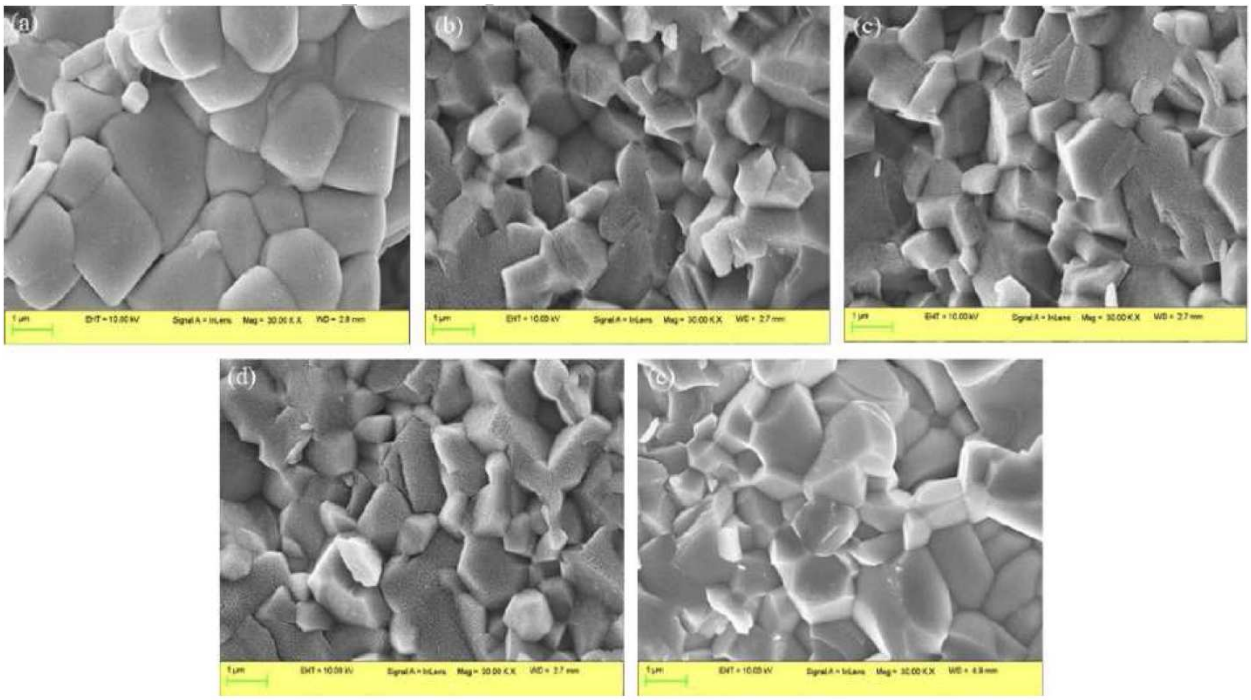

Figure 3. FESEM images of BSTO-BFTO composites: a) 90-10, b) 80-20, c) 70-30, d) 60-40 and e) 50-50

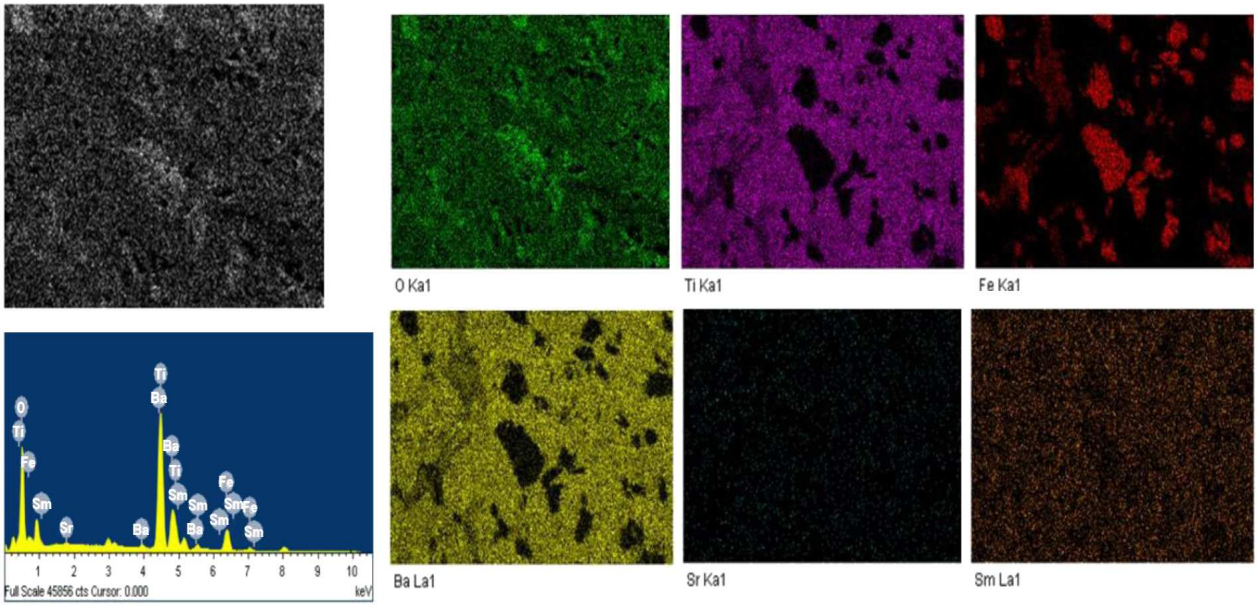

Figure 4. The mapping and EDAX for 90-10 composite

3.3. X-ray photoelectron spectroscopy

The presence of multivalent Fe ions as well as changes in their relative concentrations in prepared ceramic composites were analysed by X-ray photoelectron spectroscopy (XPS). Figure 5 displays the Fe core level spectra of the 90-10 and 50-50 composites. The peaks at core level are rather wide and exhibit asymmetry towards higher energy side, suggesting existence of multiple peaks. With the assumption of the Gaussian peak profile, peak deconvolution was performed using XPSPEAK 4.1 software and de-convoluted data shown in Fig. 5. In deconvoluted spectra, peaks corresponding to ~709.9 and 722.5 eV show presence of Fe^{3+} whereas ~712 and ~725 eV indicate the presence of Fe^{2+} [27,28]. The peak marked with * indicates satellite peak. It has been clearly visualized in graphs that as x goes from 0.1 to 0.5, area of Fe^{3+} peak increases from 0.79 for $x = 0.1$ to 1.27 for $x = 0.5$ whereas area of Fe^{2+} peak decreases from 1.26 for $x = 0.1$ to 0.78 for $x = 0.5$ which results in the increase of magnetization. Thus, the increased Fe^{3+}/Fe^{2+} ratio with increase of x from 0.1 to 0.5 should have direct influence on improvement of magnetic behaviour and increase of saturation magnetization.

3.4. Magnetic properties

Figure 6 illustrates the magnetisation versus magnetic field (*M-H* loops) at ambient temperature for each processed sample. In addition, the values of residual magnetization, coercive field and saturation magnetization are given in Table 2. It is evident that the saturation magnetization increases progressively with the increase of x from 0.1 to 0.5. This is brought on by the hexaferrite phase's rising concentration. Thus, for the sample 90-10 the maximum magnetization (M_s) is only 5.53 emu/g, but for the 50-50 composite it is 39.98 emu/g.

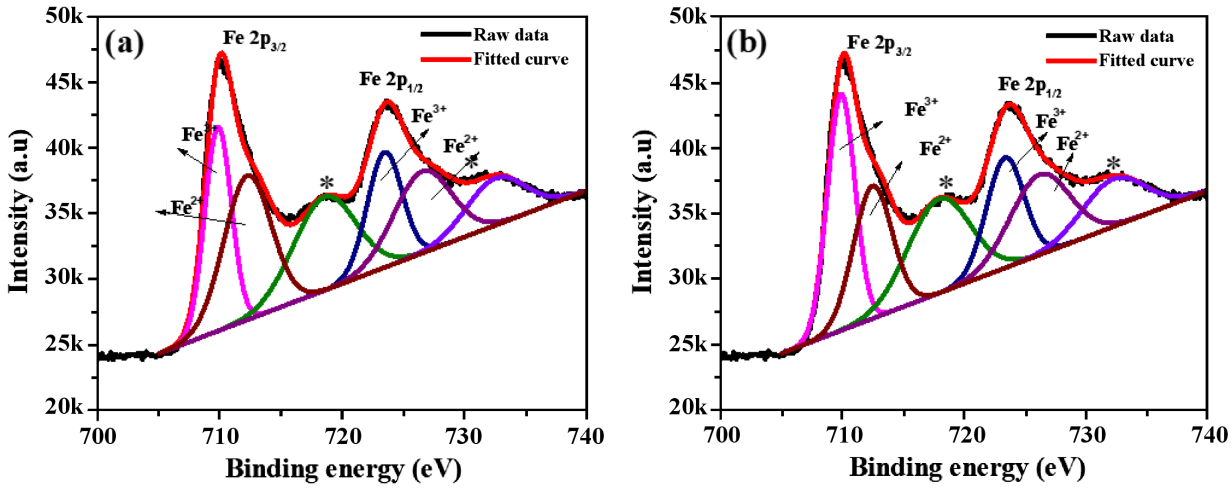

Figure 5. Deconvoluted X-ray photoelectron spectra of (a) 90-10 and (b) 50-50 composites

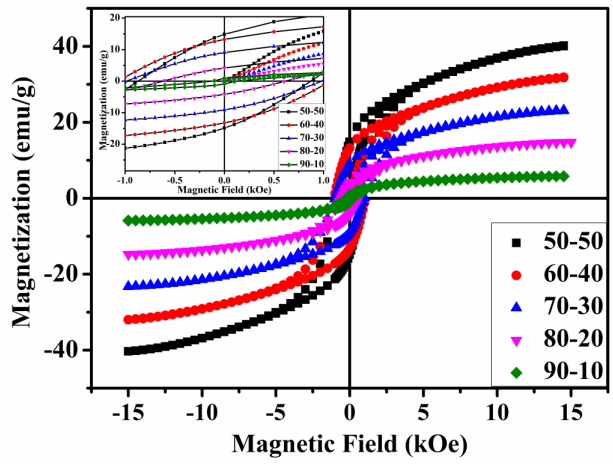

Figure 6. The magnetic strength versus field (*M-H* loops) at ambient temperature

Table 2. Remnant magnetization (M_r), maximum magnetization (M_s) and coercive field (H_c)

Sample	M_r [emu/g]	M_s [emu/g]	H_c [kOe]
90-10	0.841	5.53	0.118
80-20	4.189	14.58	0.621
70-30	9.098	23.39	0.982
60-40	13.27	31.93	1.076
50-50	14.95	39.98	0.858

An M-type hexaferrite's unit cell displays an ordered set of structuring blocks called SRS*R*S*T, in which the big Ba^{2+} cations reach a place in the oxygen lattice while the Fe^{3+} cations are dispersed among five distinct crystallographic sites, specifically the trigonal bipyramidal (2*b*), octahedral (12*k*, 2*a* and $4f_2$) and tetrahedral ($4f_1$) [29–31]. Fe^{3+} has five unpaired electrons with no pairing in their 3*d* orbital spaces, and each one of them has a 5 μ_B magnetic moment. This magnitude of moment is associated with the magnetic character of hexaferrite [29–32]. Therefore, with increase in hexaferrite content, the magnetic character of the composite samples rises.

3.5. Magneto-dielectric coupling

Magneto-dielectric coupling integrity was assessed for each sample using ε' versus frequency measurements at various magnetic fields (0, 0.4, 0.8 and 1.2 T), as shown in Fig. 7. The samples with $x \geq 0.2$ have shown magneto-dielectric coupling because the value of ε' varies as the magnetic field changes only in these samples. The plot shows that ε' decreased noticeably for $x \geq 0.2$. Additionally, an adverse magneto-dielectric response in the samples is indicated by this decrease in ε'. Because of magnetostriction in the hexaferrite phase, the application of a magnetic field causes the ferrite cell to change shape. After that, the ferroelectric particles experience the strain, which causes an electric polarization. Thus, the change in dielectric permittivity is caused by the simultaneous creation of stress in the magnetic and ferroelectric domains by an external magnetic field [6,7]. One can compute the magneto-dielectric response (*MDR*) in the following way:

$$MDR = \frac{\varepsilon'_H - \varepsilon'_0}{\varepsilon'_0} \times 100 \quad (1)$$

where the dielectric permittivity with and without a magnetic field are represented by ε'_H and ε'_0, respectively.

Figure 8 presents the *MDR* values for each specimen at frequency of 100 Hz and room temperature. The response values indicate that the highest magneto-

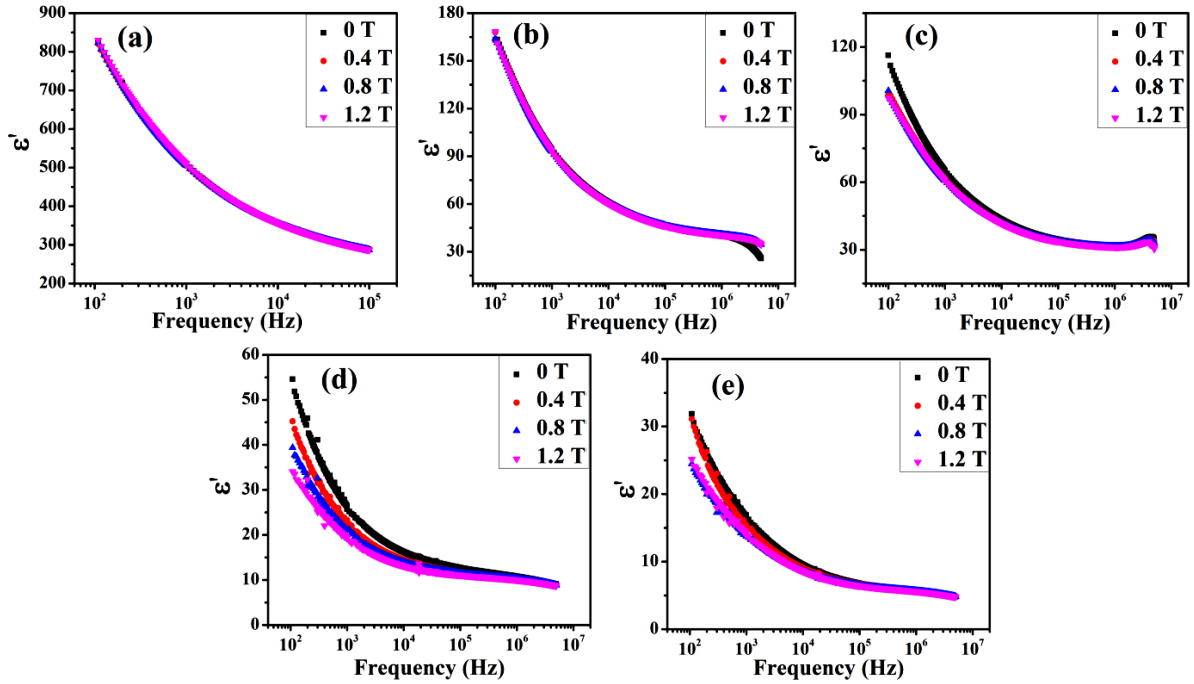

Figure 7. ε' vs. frequency at different magnetic fields for: a) 90-10, b) 80-20, c) 70-30, d) 60-40 and e) 50-50 composites

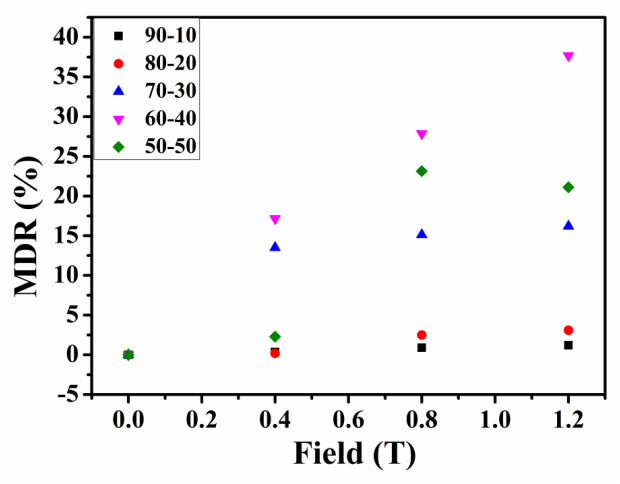

Figure 8. *MDR* values for every specimen at frequency of 100 Hz and room temperature

dielectric effect can be obtained for the sample 60-40 (i.e. $x = 0.4$). Thus, the highest interaction of the BSTO phases' electric domains and the hexaferrite's magnetic domains is characteristic of the sample 60-40 and its weakening is caused by further rise of hexaferrite phase content.

3.6. Magnetoelectric coupling coefficient

The presence of magnetoelectric coupling in the (1-x)$Ba_{0.98}Sm_{0.02}TiO_3$-$xBa_{0.7}Sr_{0.3}Fe_{12}O_{19}$ ceramics was analysed by measurement of α vs. frequency in the presence of AC magnetic field (Fig. 9). The change in voltage with application of AC magnetic field as frequency increases is caused by the presence of magnetoelectric coupling in the prepared ceramic samples.

The frequency voltage sweep was carried out to find optimal frequency at which prepared ceramic sample exhibits maximum change in voltage as frequency increases with magnetic field of ~20 Oe. ME coupling coefficient was calculated by the following formula:

$$\alpha = \frac{\mathrm{d}E}{\mathrm{d}H} = \frac{1}{d}\frac{\mathrm{d}V}{\mathrm{d}H} = \frac{V_{out}}{h_0 \cdot d} \qquad (2)$$

where V_{out}, H, h_0 and d have their general meanings. The required AC magnetic field was initiated with lock-in-amplifier and common mode induction contribution in differential mode used to calculate induced voltage. It has been clearly observed from the Fig. 9a that in frequency range from 170–220 Hz, prepared 90-10 ceramic composite exhibits maximum change in α.

The ME coefficient α first increases from 0.13 to 0.15 mV/cm·Oe and then decreases in the sample 90-10 (Fig. 9a). However, in the sample 50-50 it decreases continuously with increase in frequency (Fig. 9b). The exchange interaction due to antiferromagnetic compounds results into ME coupling in multiferroics [33–36], whereas local interaction between spin moments with disordered electric dipoles is responsible for ME coupling in titanate based multiferroics.

For further interpretation of ramifications of applied magnetic field on magnetoelectric coupling coefficient, α vs. magnetic field for all samples at frequencies 180, 200 and 220 Hz, selected from frequency sweep, are shown in Fig. 10.

It has been clearly depicted from graph that, in both ceramic composites, α continuously increases with increase in both magnetic field and frequency but for $x = 0.1$, α exhibits maximum value of 0.13 mV/cm·Oe at frequency of 220 Hz as compared with 0.0375 mV/cm·Oe at 220 Hz for the sample 50-50. Therefore, it can be concluded that the sample with $x = 0.1$ shows maximum value of α becoming important candidate for various magnetoelectric applications.

IV. Conclusions

Solid-state reaction method was used to prepare $Ba_{1-x}Sm_xTiO_3$ powders, while $Ba_{1-x}Sr_xFe_{12}O_{19}$ powders were synthesized by sol-gel auto combustion route. The selected titanate and M-type hexaferrite powders were used for fabrication of (1-x)$Ba_{0.98}Sm_{0.02}TiO_3$-$xBa_{0.7}Sr_{0.3}Fe_{12}O_{19}$ composites (x = 0.1, 0.2, 0.3, 0.4, and 0.5) by their mixing, compaction and sintering at 1240 °C. The hexaferrite and perovskite phases were

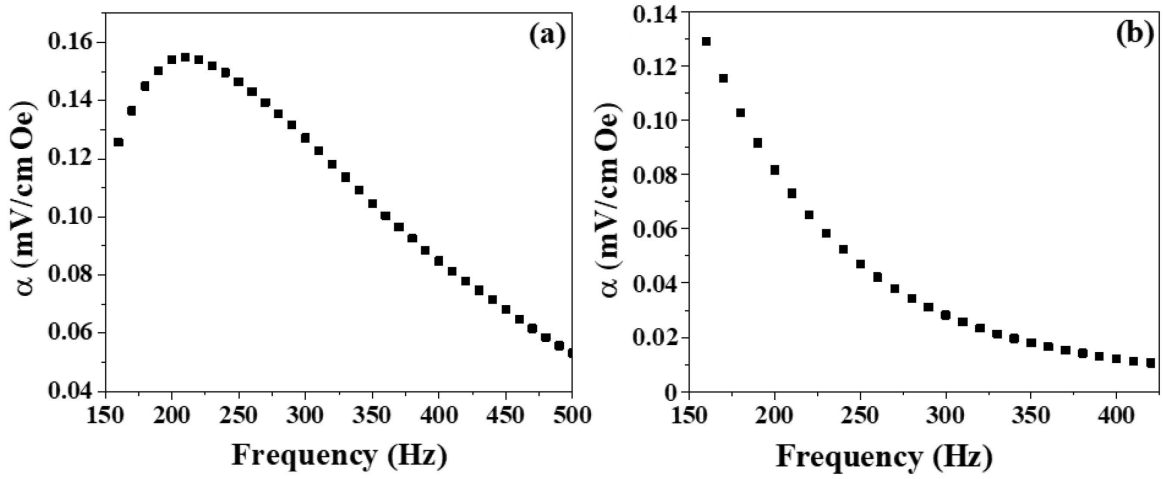

Figure 9. Magnetoelectric coefficient (α) vs. frequency (at AC magnetic field of ~20 Oe) for: a) 90-10 and b) 50-50 ceramics

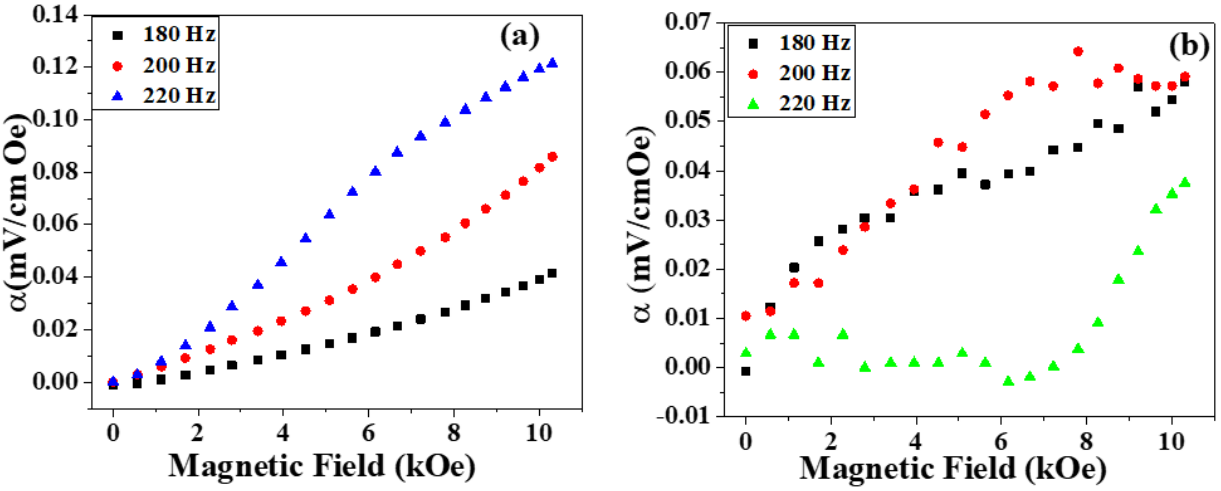

Figure 10. Magnetoelectric coefficient (α) vs. magnetic field for: a) 90-10 and (b) 50-50 ceramics

confirmed by XRD results. The maximum magnetization rises (from 5.53 to 39.98 emu/g) with an increase in content of hexaferrite phase, which is correlated with the Fe^{3+} content (determined by XPS analyses). The samples with $x \geq 0.2$ showed magnetodielectric coupling and the highest MDR value of 37.68% was measured for the sample with $x = 0.4$ (at magnetic field of 1.2 T and frequency of 100 Hz). In addition, maximum change of magnetoelectric coefficient α (of 0.13 mV/cm·Oe at frequency of 220 Hz) was observed for the composite sample 0.9BSTO-0.1BSFO with $x = 0.1$.

Acknowledgements: The authors would like to thank Centre for Emerging Life Sciences, GNDU for providing characterization facilities (FESEM and VSM). Arshdeep Kaur is thankful for financial support in the form of DST-INSPIRE Fellowship (DST/INSPIRE/Fellowship/2021/IF210379) by the Department of Science and Technology (DST), Ministry of Science and Technology, Government of India. One of the authors (Sajan Masih) would like to thank UGC-DAE CSR for providing financial support.

References

1. N.A. Hill, A. Filippetti, "Why are there any magnetic ferroelectrics?", *J. Magn. Magn. Mater.*, **242-245** (2002) 976–979.
2. C.W. Nan, M.I. Bichurin, S. Dong, D. Viehland, G. Srinivasan, "Multiferroic magnetoelectric composites: Historical perspective, status, and future directions", *J. Appl. Phys.*, **103** (2008) 031101.
3. D.I. Khomskii, "Multiferroics: Different ways to combine magnetism and ferroelectricity", *J. Magn. Magn. Mater.*, **306** [1] (2006) 1–8.
4. N.A. Spaldin, M. Fiebig, "The renaissance of magnetoelectric multiferroics", *Science*, **309** [5733] (2005) 391–392.
5. W. Eerenstein, N.D. Mathur, J.F. Scott, "Multiferroic and magnetoelectric materials", *Nature*, **442** (2006) 759–765.
6. S.R. Kulkarni, C.M. Kanamadi, K.K. Patankar, B.K. Chougule, "Magnetic properties and magnetoelectric effect in $Ni_{0.8}Co_{0.1}Cu_{0.1}Fe_2O_4$ + $PbZr_{0.2}Ti_{0.8}O_3$ composites", *J. Mater. Sci.*, **40** (2005) 5691–5694.
7. C.W. Nan, "Magnetoelectric effect in composites of piezoelectric and piezomagnetic phases", *Phys. Rev. B*, **50** (1994) 6082–6088.
8. M. Rawat, K.L.Yadav, "Electrical, magnetic and magnetodielectric properties in ferrite-ferroelectric particulate composites", *Smart Mater. Struct.*, **24** (2015) 45041.
9. K. Aggarwal, M. Sharma, S. Kaur, V. Arora, I. Sharma, R. Kumar, A. Singh, "Establishment of magneto-dielectric effect and magneto-resistance in composite of PLT and Ba-based U-type hexaferrite", *J. Adv. Dielectr.*, **13** [5] (2023) 2350013.
10. B. Ertuğ, "The overview of the electrical properties of barium titanate", *Am. J. Eng. Res.*, **2** (2013) 1–7.
11. K. Tewatia, A. Sharma, M. Sharma, A. Kumar "Factors affecting morphological and electrical properties of barium titanate: A brief review", *Mater. Today Proc.*, **44** (2020) 4548–4556.
12. W. Cai, C. Fu, J. Gao, X. Deng, G. Chen, Z. Lin, "Effect of samarium on the microstructure, dielectric and ferroelectric properties of barium titanate ceramics", *Integr. Ferroelectr.*, **140** (2012) 92–103.
13. H. Kishi, Y. Mizuno, H. Chazono, "Base-metal electrode-multilayer ceramic capacitors: Past, present and future perspectives", *Jpn. J. Appl. Phys.*, **42** [1R] (2003) 1–15.
14. R. Joshi, C. Singh, D. Kaur, H. Zoki, S. Bindra Narang, R. Jotania, S.R. Mishra, J. Singh, P. Dhruv, M. Ghimire, "Structural and magnetic properties of Co^{2+}-W^{4+} ions doped M-type Ba-Sr hexaferrites synthesized by a ceramic method", *J. Alloys Compd.*, **695** (2017) 909–914.
15. S.V. Trukhanov, A.V. Trukhanov, V.G. Kostishyn, L.V. Panina, An.V. Trukhanov, V.A. Turchenko, D.I. Tishkevich, E.L. Trukhanova, O.S. Yakovenko, L.Yu. Matzui, D.A. Vinnik, D.V. Karpinsky, "Effect of gallium doping on electromagnetic properties of barium hexaferrite", *J. Phys. Chem. Solids*, **111** (2017) 142–152.
16. S. Wang, C. Zhang, R. Guo, L. Lu, Y. Yang, K. Li, "Preparation and properties of yttria doped tetragonal zirconia polycrystal/Sr-doped barium hexaferrite ceramic composites", *Mater. Sci. Eng. B*, **193** (2015) 91–96.

17. M.J. Iqbal, S. Farooq, "Impact of Pr-Ni substitution on the electrical and magnetic properties of chemically derived nanosized strontium-barium hexaferrites", *J. Alloys Compd.*, **505** (2010) 560–567.
18. Z. Mosleh, P. Kameli, A. Poorbaferani, M. Ranjbar, H. Salamati, "Structural, magnetic and microwave absorption properties of Ce-doped barium hexaferrite", *J. Magn. Magn. Mater.*, **397** (2016) 101–107.
19. V.R. Palkar, D.C. Kundaliya, S.K. Malik, S. Bhattacharya, "Magnetoelectricity at room temperature in the $Bi_{0.9-x}Tb_xLa_{0.1}FeO_3$ system", *Phys. Rev. B.*, **69** (2004) 212102.
20. M. Kumar, K.L. Yadav, "Study of dielectric, magnetic, ferroelectric and magnetoelectric properties in the $PbMn_xTi_{1-x}O_3$ system at room temperature", *J. Phys. Condens Matter.*, **19** (2007) 242202.
21. K. Parida, S. Kumar Dehury, R.N.P. Choudhary, "Structural, electrical and magneto-electric characteristics of complex multiferroic perovskite $Bi_{0.5}Pb_{0.5}Fe_{0.5}Ce_{0.5}O_3$", *J. Mater. Sci. Mater. Electron.*, **27** (2016) 11211–11219
22. K. Jyotsna, M. Tomar, S. Phanjoubam "Strong magnetoelectric coupling in novel $Na_{0.5}Bi_{0.5}TiO_3$-$BaFe_{12-2x}Co_xTi_xO_{19}$ multiferroic composite", *Ceram. Int.*, **50** (2024) 33189–33202.
23. E. Arya, A. Agarwal, R. Dhar, S. Sanghi, M. Chauhan, V. Vermani, P. Sharma, S. Kaushik, "Structural, dielectric and magnetic properties of Ca doped barium hexaferrite-$Na_{0.5}Bi_{0.5}TiO_3$ magneto-electric composites", *Mater. Today Proc.*, **82** (2023) 145–150.
24. D.R. Patil, B.K. Chougule "Structural, electrical and magnetic properties of $xNiFe_2O_4$+(1-x)$Ba_{0.8}Sr_{0.2}TiO_3$ ME composites", *J. Alloys Compd.*, **458** (2008) 335–339.
25. A. Kumari, K. Kumari, F. Ahmed, A. Alshoaibi, P.A. Alvi, S. Dalela, M.M. Ahmad, R.N. Aljawfi, P. Dua, A. Vij, S. Kumar, "Influence of Sm doping on structural, ferroelectric, electrical, optical and magnetic properties of $BaTiO_3$", *Vacuum*, **184** (2021) 109872.
26. S. Anjum, S. Hameed, M.S. Awan, E. Amed, A. Sattar, "Effect of strontium doped M-type bariam hexa-ferrites on structural, magnetic and optical properties", *Optik*, **131** (2017) 977–985.
27. J. Meng, N. Yuan, X. Liu, C. Yao, F. Meng, X. Niu, X. Wu, J. Meng, "Assessment of $LaM_{0.25}Mn_{0.75}O_{3-\delta}$ (M = Fe, Co, Ni, Cu) as promising cathode materials for intermediate-temperature solid oxide fuel cells", *Electrochim. Acta*, **169** (2015) 264–275.
28. Y. Wang, C. Nan, "Enhanced ferroelectricity in Ti-doped multiferroic $BiFeO_3$ thin films enhanced ferroelectricity in Ti-doped multiferroic $BiFeO_3$ thin films", *Appl. Phys. Lett.*, **89** (2006) 052903.
29. D.M. Chandra, H. Khanduri, H. Kooskora, I. Heinmaa, E. Joon, R. Stern, "Magnetic properties and ^{57}Fe NMR studies of U-type hexaferrites", *J. Magn. Magn. Mater.*, **323** (2011) 2210–2213.
30. P.S. Malhi, S. Kumar, M. Singh, A. Singh, A.K. Sood, "Finite control of dielectric constant with magnetic field in Sm-doped Ba-Co U-type hexaferrites", *Process. Appl. Ceram.*, **17** [4] (2023) 333–346.
31. S. Ounnunkad, "Improving magnetic properties of barium hexaferrites by La or Pr substitution", *Solid State Commun.*, **138** (2006) 472–475.
32. J. Jia, C. Liu, N. Ma, G. Han, W. Weng, P. Du, "Exchange coupling controlled ferrite with dual magnetic resonance and broad frequency bandwidth in microwave absorption", *Sci. Technol. Adv. Mater.*, **14** [4] (2013) 045002.
33. S.N. Babu, K. Srinivas, T. Bhimasankaram, "Studies on lead-free multiferroic magnetoelectric composites", *J. Magn. Magn. Mater.*, **321** (2009) 3764–3770.
34. R.S. Devan, D.R. Dhakras, T.G. Vichare, A.S. Joshi, S.R. Jigajeni, Y.R. Ma, B.K. Chougule, "$Li_{0.5}Co_{0.75}Fe_2O_4$ + $BaTiO_3$ particulate composites with coupled magnetic-electric properties", *J. Phys. D Appl. Phys.*, **41** [10] (2008) 105010.
35. G. Sreenivasulu, J. Zhang, R. Zhang, M. Popov, V. Petrov, G. Srinivasan, "Multiferroic core-shell nanofibers, assembly in a magnetic field, and studies on magneto-electric interactions", *Materials*, **11** [1] (2018) 18.
36. F.L. Zabotto, V.F. Barbosa, C.C.S. Pereira, F.R. Estrada, M.H. Lente, X.M. Chen, J.A. Eiras, "Distinct magnetic contributions for magnetoelectric coupling at room temperature in perovskite PZT-PFN solid solutions", *J. Alloys Compd.*, **929** (2022) 167271.